

Concealing Backdoor Model Updates in Federated Learning by Trigger-Optimized Data Poisoning

Yujie Zhang
Duke University
yujie.zhang396@duke.edu

Neil Gong
Duke University
neil.gong@duke.edu

Michael K. Reiter
Duke University
michael.reiter@duke.edu

Abstract

Federated Learning (FL) is a decentralized machine learning method that enables participants to collaboratively train a model without sharing their private data. Despite its privacy and scalability benefits, FL is susceptible to backdoor attacks, where adversaries poison the local training data of a subset of clients using a backdoor trigger, aiming to make the aggregated model produce malicious results when the same backdoor condition is met by an inference-time input. Existing backdoor attacks in FL suffer from common deficiencies: fixed trigger patterns and reliance on the assistance of model poisoning. State-of-the-art defenses based on Byzantine-robust aggregation exhibit a good defense performance on these attacks because of the significant divergence between malicious and benign model updates. To effectively conceal malicious model updates among benign ones, we propose DPOT, a backdoor attack strategy in FL that dynamically constructs backdoor objectives by optimizing a backdoor trigger, making backdoor data have minimal effect on model updates. We provide theoretical justifications for DPOT’s attacking principle and display experimental results showing that DPOT, via only a *data*-poisoning attack, effectively undermines state-of-the-art defenses and outperforms existing backdoor attack techniques on various datasets.

1 Introduction

Federated Learning (FL) is a decentralized machine-learning approach that has gained widespread attention for its ability to address various challenges. Unlike traditional centralized model training, FL enables model updates to be computed locally on distributed devices, offering enhanced data privacy, reduced communication overhead, and scalability across various domains. In FL, a central server distributes a global model to participating clients, each of whom independently trains the model on their local data, and their model updates are aggregated by the server over multiple rounds.

Despite its advantages, FL has been proven susceptible to backdoor attacks [1]. Backdoor attacks in fed-

erated learning involve adversaries inducing the local models of a subset of clients to learn backdoor information carried by triggers and strategically integrating these backdoored local models into the global model. Ultimately, the global model will generate the adversary-desired result when the same trigger conditions are met. In this work, we term clients manipulated by adversaries during local training as *malicious clients*, and those unaffected as *benign clients*.

Existing backdoor attacks in FL present two common deficiencies. First, the patterns of backdoor triggers are pre-defined by the attacker and remain unchanged throughout the entire attack process [1, 33, 29, 13]. Consequently, the optimization objective brought by backdoored data (backdoor objective) is static and incoherent with the optimization objective of main-task data (benign objective), resulting in distinct differences in model updates after training. These malicious clients’ model updates are therefore easily canceled out by robust aggregations [1, 38, 13]. Second, many approaches rely on model-poisoning techniques to enhance the effectiveness of backdoor attacks. These model-poisoning techniques involve (i) strategically scaling up the malicious clients’ model updates with a carefully chosen factor to overpower the benign clients’ model updates during aggregation [1, 29, 33], and (ii) restricting the malicious clients’ model updates from deviating significantly from the benign clients’ model updates by modifying the loss function [1, 9, 3] (e.g., adding restriction terms) or changing the optimization algorithm [2, 31] (e.g., employing gradient projection method in optimization). Implementing model-poisoning attacks requires attackers to change the training procedures of a certain number of genuine clients (e.g., at least 20% of all clients [2, 9, 31]) to make their local training algorithms different from other clients. However, achieving this condition is challenging, as advanced defense mechanisms [24] have introduced Trusted Execution Environments (TEEs) to ensure the secure execution of client-side training, making it harder to adopt suspicious modifications to the training procedure.

Existing defenses against backdoor attacks in FL (see more details in Section 2.3) rely on a hypothesis that

backdoor attacks will always cause the updating direction of a model to deviate from its original benign objective, because the backdoor objectives defined by backdoored data cannot be achieved within the original direction. However, the capabilities of backdoor attacks are not limited to this hypothesis. To counter this hypothesis, adversaries can align the updating directions of a model with respect to backdoor and benign objectives by strategically adjusting the backdoor objective. Applying this idea to FL, if the injection of backdoored data has minimal effect to the updates of a client’s model, then detecting this client as malicious becomes challenging for defenses that analyze its model updates, gradients, or neuron behavior.

In this work, we propose **Data Poisoning with Optimized Trigger (DPOT)**, a backdoor attack on FL that dynamically constructs a backdoor objective to constantly minimize the divergence between malicious clients’ model updates with benign clients’ model updates for each round of FL training. We construct the backdoor objective by optimizing the backdoor trigger that is used to poison malicious clients’ local data. Without any assistance of model-poisoning techniques, malicious clients can effectively conceal their model updates among benign clients’ model updates by simply executing a normal training process on their poisoned local data, and render state-of-the-art defenses ineffective in mitigating our backdoor attack.

The optimization of the backdoor trigger in each round is independent and specific to the current round’s global model. The objective of this optimization is to generate a trigger such that the current round’s global model exhibits minimal loss on backdoored data having this trigger. Once the global model becomes optimal for the backdoored data, further training on the backdoored data will result in only minor model updates to the global model within a limited number of local training epochs. Therefore, when a malicious client’s local dataset is partially poisoned by the optimized trigger while the rest remains benign, the model updates produced by training on the local data will be dominated by benign model updates. We provide theoretical and experimental justifications for the sufficiency of trigger optimization in minimizing the difference between a malicious client’s model updates and those of benign clients.

In order to enhance the practicality of our attack, in our experiments we limited the trigger size to a reasonable level, ensuring it cannot obscure essential details of the original data, allowing for accurate recognition by humans. To meet this constraint, we developed two algorithms to optimize the locations and values of trigger pixels respectively. To the best of our knowledge, we are the first to generate an optimized trigger with arbitrary shape and location while specifying its exact size.

We evaluated DPOT on four image data sets (Fashion-MNIST, FEMNIST, CIFAR10, and Tiny ImageNet) and four model architectures including ResNet and VGGNet. We tested the attack effectiveness of DPOT under a variety of defense conditions—nine different defense strategies in FL including state-of-the-art defenses for backdoor attacks such as Robust Federated Aggregation [23] (RFA), FLAME [22], FLAIR [27], FLCert [7], and Fools-gold [12]—and compared it with three existing data-poisoning backdoor attacks that employ fixed-pattern triggers, distributed fixed-pattern triggers [33], and triggers optimized by a state-of-the-art attack method [37], respectively. Using a small number of malicious clients (5% of the total), DPOT outperformed existing data-poisoning backdoor attacks in effectively undermining defenses without affecting the main-task performance of the FL system.

In summary, our contributions are as follows:

- We propose a novel backdoor attack mechanism, DPOT, in FL that effectively conceals malicious client’s model updates among those of benign clients by dynamically adjusting backdoor objectives, and demonstrate that existing defenses focusing on detecting outlier model updates by analyzing information related to clients’ model parameters (or neurons) are inadequate.
- We dynamically construct backdoor objectives by optimizing a backdoor trigger and injecting it to client’s data, which does not rely on additional assistance from model-poisoning techniques.
- We offer both theoretical and experimental justifications for the adequacy of our trigger optimization in reducing the disparity between model updates from malicious clients and those from benign clients.
- We develop algorithms to optimize a trigger, allowing for flexibility in its shape, location, and value, while also specifying its precise size.
- We extensively evaluate our attack on four benchmark datasets, showing that DPOT achieves better attack effectiveness than three advanced data-poisoning backdoor attacks in compromising nine state-of-the-art defenses in FL.

2 Related Work

2.1 Federated Learning (FL)

The Federated Learning [21] (FL) training process involves four main steps: 1) **Model Distribution**: A central server distributes the most recent global model to the participating clients. 2) **Local Training**: Each client independently trains the global model on its local

training dataset and obtains a local model. 3) **Model Updates**: Each client calculates the parameter-wise difference between its local model and the global model, referred to as model updates, and then sends them to the central server. 4) **Aggregation**: The central server aggregates clients’ model updates to create a new global model. This entire process, consisting of step 1 to 4, constitutes a global round. The FL system repeats these steps for a certain number of rounds to obtain a final version of the global model.

2.2 Backdoor Attacks in FL

A brief introduction of backdoor attacks: Backdoor attack in machine learning is a security vulnerability where an adversary manipulates a model’s behavior by making it learn some trigger information, causing the model to produce erroneous results when trigger conditions are met. Meanwhile, the backdoor attack also ensures that the model maintains normal performance on benign data to evade detection. In image classification tasks, a backdoor attack aims to manipulate a model so that it classifies any image containing a specific pixel-pattern trigger into a label chosen by the attacker [8, 14, 16, 18, 35, 30, 19].

Backdoor triggers with fixed pattern: Backdoor attack has been regarded as a primary security threat in FL since its initial discussion in the context of FL [1]. State-of-the-art backdoor attacks to FL involve the following two categories of triggers: 1) **Semantic Backdoor** [1]: Attackers exploit shared characteristics among different data, such as an unusual car color (e.g., green), to serve as the trigger information. 2) **Artificial Backdoor** [33, 29, 13]: Attackers artificially introduce patterns that do not naturally exist in the main-task data to serve as the trigger information (e.g. pixels with a specific pattern embedded in images). In this category, three types of triggers exist: Single Global Trigger [29], where all malicious clients inject the same trigger into their local data; Distributed Trigger [33], which decomposes the global trigger into many local triggers and assign them to the corresponding compromised participants; and Coordinated Trigger [13], similar to Distributed Trigger but with malicious clients generating their own local triggers to form a global trigger.

A commonality among these studies is that the patterns of the backdoor triggers are pre-defined by the attacker and remain unchanged throughout the entire attack process. Therefore, the optimization objectives brought by backdoored data keep static and incoherent with the optimization objective of main-task data, resulting that malicious clients’ models have distinct differences in their model updates compared to those of benign clients. The deviated model updates are eas-

ily canceled out by robust-aggregation and then the global model will quickly forget the backdoor information [1, 38, 13]. In this work, we focus on developing and evaluating attacks within the scope of Artificial Backdoor, because this type of attack can be applied to any data, eliminating the need for assumptions about the content of malicious clients’ data.

Data poisoning vs. model poisoning to FL: In conducting backdoor attacks in FL, attackers embed backdoor triggers into the local training data of certain clients and manipulate the ground-truth labels of the infected data to match a targeted label defined by attackers. This process is known as “data poisoning”. Malicious clients train their local models on their poisoned datasets to produce backdoored models. When the global model aggregates these backdoored models, it also acquires the backdoor information carried by the poisoned data, leading to the production of malicious results.

However, due to the limitations of employing fixed-pattern triggers in backdoor attacks, a standalone data poisoning is challenging to achieve significant attack effectiveness in FL. Therefore, many works have suggested combining “data poisoning” and “model poisoning” techniques to enhance the effect of backdoor attacks, where the “model poisoning” aims to either directly manipulate model parameters or indirectly achieve this by changing model training algorithm. The state-of-the-art model-poisoning techniques can be summarized into two main categories: 1) **Scaling based** [1, 29, 33]: Attackers intensify the backdoor effect by strategically scaling up the malicious clients’ model updates with a carefully chosen factor to overpower the benign model updates during aggregation. However, given the emergence of FL defenses employing clipping and restricting methods during the aggregation process, the effect of straightforward scaling has been effectively mitigated. 2) **Constraint based** [1, 29, 3, 2, 31]: A stealthier model-poisoning technique is to restrict the malicious clients’ model updates from diverging too much from those of benign clients. Some authors (e.g., [1, 3]) proposed to modify the optimization objective (loss function) by adding restriction terms (e.g., L2-norm distance to the global model). Baruch, et al. [2] and Wang, et al. [31] introduce the projected gradient descent (PGD) optimization technique to project a malicious model’s parameters onto a small range centered around the current-round global model’s parameters, which also prevents its model updates diverge largely from other clients’ model updates.

Model poisoning requires attackers to modify certain clients’ local training procedures to distinguish them from others. However, with the introduction of Trusted Execution Environments (TEEs) by state-of-the-art de-

fense mechanisms [24], client-side execution for training can be authenticated and secure, thus increasing the difficulty of conducting model poisoning. Compared to model poisoning, data poisoning is easier to conduct and harder to prevent since clients may collect their local data from open resources where attackers can also get access to and make modifications. For example, autonomous driving vehicles collect their data on road traffic signage [34] from real world, and attackers can easily place stickers on traffic signage objects to inject backdoor trigger information. Hence, we view data poisoning as the primary threat to an FL system.

Trigger optimization in backdoor attacks: In recent state-of-the-art studies on backdoor attacks in Federated Learning, optimized triggers have been found to be highly effective in compromising clients’ local models and thus are used in data poisoning. However, these studies suffer from deficiencies such as incorrectly defining backdoor triggers, setting hypothesis-based objectives for trigger optimization, or insufficiently optimizing triggers. Consequently, the optimized triggers used in existing studies do not convincingly demonstrate attack effectiveness on global models solely through data poisoning, leading these studies to rely on other techniques to enhance attack effectiveness.

CerP [20] proposed to add carefully optimized perturbations to malicious clients’ local data to induce their local models misclassify the perturbed data to a specified target label. However, this approach contradicts the common understanding of injecting backdoor triggers, as the perturbations, which make small changes to original image pixels, do not introduce consistent external features across different images. A backdoor trigger considered in this work should entirely replace certain pixels of images with its own pattern, enabling the model to learn associations between trigger features and target labels. Additionally, CerP relies on model-poisoning techniques to conduct unfaithful training with malicious objectives (e.g. adding regularization to limit the cosine similarity between each pairwise malicious models), making it can not survive in TEEs.

We recognize A3FL [37] and model-dependent trigger [13] are two works that correctly design optimized backdoor triggers in backdoor attacks on FL, while their objectives of trigger optimization are established differently. A3FL indicates that triggers optimized for local models can not achieve similar effectiveness when transferred to the global model due to the local-global gap, which does not accord with our experiment results. To address this “limitation”, A3FL optimizes triggers concurrently with updating the local model by unlearning the optimized triggers and repeating this two steps back and forth. However, there is no evidence demonstrating that the local model, after unlearning the backdoor trig-

gers, will have a smaller gap to the next-round global model in general cases. Model-dependent triggers [13] are optimized to maximize the activation of certain neurons inside the local model, but it is unclear how this contributes to the global model’s better learning of trigger information. Unfortunately, we were unable to find any available code, pseudocode, or algorithms to guide us in replicating model-dependent triggers and their results.

The last deficiency existing in state-of-the-art works is that their optimizations on backdoor trigger are insufficient so that they do not fully exploit the potential of optimized triggers in attacks. Specifically, existing works are concentrated on optimizing trigger values while keeping trigger placement and shape fixed. In our experiments, we show that DPOT triggers outperform A3FL [37]’s triggers in data-poisoning attacks on FL, proving that placement and shape of triggers are critical factors in improving attack effectiveness.

Clean-label attacks: Clean-label attacks [26] involve manipulating input data with subtle perturbations while keeping labels unchanged. Although this assumption aligns with scenarios like Vertical Federated Learning [32] (VFL), where participants possess vertically partitioned data with labels owned by only one participant, our study does not consider VFL as our attack scenario. Furthermore, we focus on examining the effects of different backdoor triggers on hiding malicious model updates rather than their imperceptible characteristics. Therefore, discussions of clean-label attacks are beyond the scope of our work.

2.3 Defenses against backdoor attacks in FL

Leveraging the limitations of existing attacks that use fixed-pattern triggers or scale up malicious clients’ model updates, both of which enlarge the distinction between malicious clients’ model updates and benign clients’ model updates. By analyzing information related to clients’ models such as their model updates [27, 17, 6, 22], model gradients [12], or neuron behavior [24], many defense strategies have been proposed to detect and filter out suspicious clients, and employ Byzantine-robust aggregation rules [36, 4, 23] to compute the global model updates from the remaining submissions. The following is detailed introduction to the techniques used in state-of-the-art defense works.

Byzantine-robust aggregation rules: Most defense strategies against backdoor attacks in FL design Byzantine-robust aggregation rules for the central server. Several common techniques used in state-of-the-art defenses within this category include: 1) **Parameter-wise computation** [36, 22]: The cen-

tral server aggregates model updates per parameter. This can involve computing the median or trimmed mean value of each parameter [36], or clipping and averaging model updates in a specific cluster [22]. 2) **Factor rescaling** [4, 12, 6, 27, 23]: The central server adjusts the aggregation factor of each client according to any of following reasons: the similarity of the coefficient signs with the previous round global model updates [27], the distance to the geometric median of all clients’ model updates [23], or cosine similarity with other clients’ model updates [12, 4] or with the server’s self-trained model (the server in FLTrust [6] is permitted to hold a certain amount of Main-task data from clients, which contradicts the FL goal of preserving clients’ data privacy). 3) **Clustering** [7, 22]: Prior to aggregation, the central server clusters clients’ model updates either randomly [7] or based on their cosine similarity to each other. This approach enhances the likelihood of having benign model updates as reference for the inference and aggregation process. 4) **Perturbation** [22]: The central server adds perturbation noise to the post-aggregation global model to mitigate the impact of malicious updates integrated into the global model [22].

However, employing Byzantine-robust aggregation rules as defense strategy against backdoor attacks in FL depends on a hypothesis that malicious clients’ model updates exhibit significant divergence from benign clients’ model updates. In this work, we will show our attack can effectively undermine these defenses, highlighting the limitation of this hypothesis.

Provably robust FL: FLCert [7] introduces a technique to attain “certified accuracy”, ensuring guaranteed benign testing accuracy under arbitrary attacks. However, this guarantee only applies when a small number of malicious clients exist within a much larger client population in FL. Our experiment results show that FLCert can’t sustain backdoor attacks in FL with only 5% malicious client rate.

Cross-Client Validation: CrowdGuard [24] proposes switching clients’ local models via a central server within Trusted Execution Environments (TEEs), allowing clients to analyze changes in other clients’ models using their local data and identify poisoned models through majority votes. However, this defense relies on the hypothesis that malicious models trained on backdoored datasets exhibit differences in their parameters compared to benign models, leading to abnormal output in certain layers even when benign data is inputted. If a malicious model can minimize parameter changes (model updates) induced by learning backdoor data, CrowdGuard loses effectiveness as the malicious model resembles a benign one in its parameters.

3 Threat Model

Attacker’s capability: As shown in Figure 1, we assume that each FL client—even a malicious one—is equipped with trustworthy training software that conducts correct model training on the client’s local training data and transmits the model updates to the FL server. Aligning with the security settings in the state-of-the-art defense work [24], we assume that both the client training pipeline and the FL server, as well as the communication between them, faithfully serve FL’s main task training and cannot be undetectably manipulated. These properties would be achievable by executing FL training within Trusted Execution Environments (TEEs) [25, 24], for example, by applying cryptographic protections to the updates (e.g., a digital signatures) to enable the FL server to authenticate the updates as coming from the TEEs.

Due to the TEE’s protections, malicious clients are not allowed to conduct any model poisoning, such as scaling up model updates, changing the optimization algorithm used in model training, or modifying the values of model parameters. The capability of malicious clients in our attack is limited to the manipulation of their local training data that are input to their training pipelines—i.e., a data-poisoning attack. In addition, we do *not* assume the secrecy of the global model provided by the FL server, as would be typical if the model needs to be accessible outside TEEs for use in local inference tasks. As such, in each FL round, clients are granted white-box access to the global model.

Attacker’s background knowledge: In our attack, we consider the presence of malicious clients in the FL system. As discussed above, malicious clients have knowledge about the global model’s architecture and the values of its parameters in each round. Originating from initially benign clients that have been compromised, these malicious clients can access some benign local training data relevant to the main task of the FL system.

Attacker’s goals: The malicious clients aim to accomplish the following goals.

- **Effectiveness.** By convention, *Attack Success Rate* (ASR) is used to assess the effectiveness of a backdoor attack. For classification tasks, ASR is defined as the accuracy of a model in classifying data embedded with a backdoor trigger into a target label associated with this trigger. The effectiveness goal of DPOT attack is to enable the global model in each FL round to misclassify data embedded with the backdoor trigger generated from the previous round by our algorithms, and make the global model produced at the final round of FL training achieve an ASR greater than 50%.

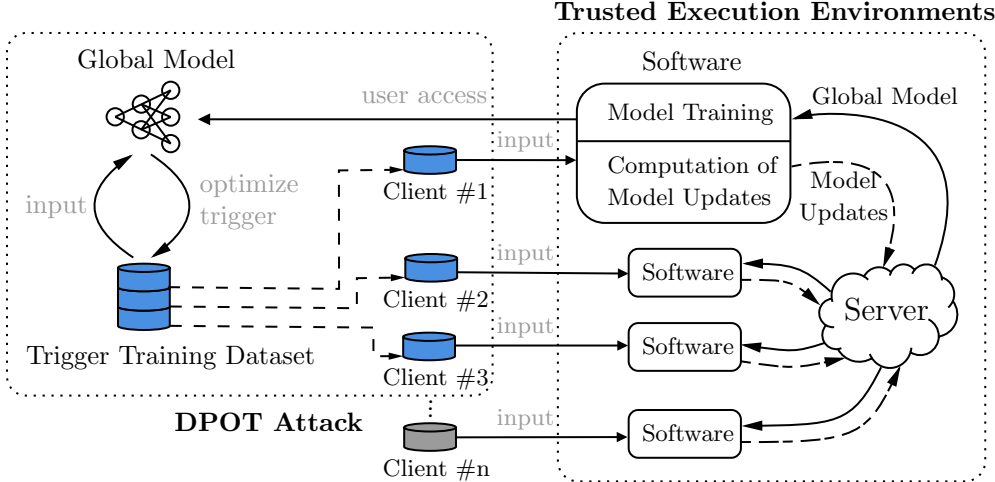


Figure 1: Overview of DPOT attack process on a FL system within Trusted Execution Environments (TEEs). In each global round of FL, DPOT attack comprises three key stages: the construction of a Trigger Training Dataset, Trigger Optimization, and the Data Poisoning to the malicious clients. In this figure, Client #1, #2, and #3 perform as the malicious clients while other clients (e.g. Client #n) are benign clients.

- **Stealthiness.** The stealthiness goal of a backdoor attack is to maintain the *Main-task Accuracy* (MA) of the global model at a normal level, ensuring the functionality of the global model on its main-task data. Specifically, we require that the compromised global model resulting from our attack has a similar MA (± 2 percentage points) compared to a global model that has not been subjected to any attacks.

4 DPOT Design

4.1 Overview

In each round of FL (e.g., the i -th round), DPOT attack takes place after the malicious clients receive the global model $W_g^{(i)}$ of this round but before they input their local training data to the trustworthy training software. Given a global model $W_g^{(i)}$ and a pre-defined target label y_t , we optimize the pattern of a backdoor trigger to increase the *ASR* of $W_g^{(i)}$. By poisoning malicious clients' local training data using this optimized trigger $\tau^{(i)}$, we expect that the global model of the next round $W_g^{(i+1)}$ will also exhibit a high ASR in classifying data embedded with $\tau^{(i)}$ into its target label y_t .

To achieve this goal, we first construct a trigger training dataset by collecting data from malicious clients. After changing the labels of all data in the trigger training dataset to be the target label y_t , we compute the gradient on each pixel of each image with respect to the loss of $W_g^{(i)}$ in misclassifying each clean image into label y_t . We determine a trigger location mask E_t in the area of an image by selecting tri_{size} number of pixels that demonstrate largest absolute values among the

pixel-wise sum of gradients from all images. Next, we optimize each pixel's value in E_t using gradient descent, obtaining the trigger value V_t . Finally, we embed the optimized trigger defined by (E_t, V_t) with its target label y_t into malicious clients' local training data at a certain poison rate.

4.2 Building a Trigger Training Dataset

At the beginning of the DPOT attack, we initially gather all available benign data from the malicious clients' local training datasets and assign a pre-defined target label y_t to them. We refer to this new dataset, which associates benign data with the target label, as the trigger training dataset D .

4.3 Optimizing Backdoor Trigger

Formulating an optimization problem: We use the trigger training dataset to generate a different backdoor trigger for each round's global model. The optimization process operates independently across the rounds of FL, implying that generating a backdoor trigger for the current round's global model does not depend on any information from previous rounds. Therefore, in this part, we introduce the trigger optimization algorithms within a single round of FL.

In the image classification context, consider the global model W_g as input and all pixels within an image as the parameter space. Our approach aims to find a subset of parameters that have the most significant impact in producing the malicious output result (i.e., target label), and subsequently optimize the values of the parameters

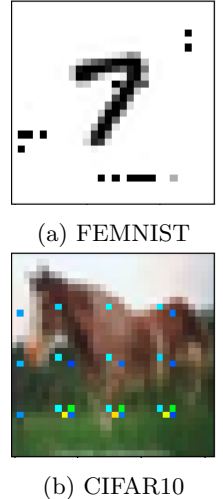


Figure 2: Poisoned data with DPOT triggers.

in this subset for the malicious objective (i.e., a high ASR). In the end, the pixels in this subset with their optimized values will serve as a backdoor trigger. This trigger will increase the likelihood that an image containing it will yield the malicious output when employing the same model W_g for inference. The optimization objective to resolve the above problem can be written as formula 1.

$$\min_{\tau} \frac{1}{|D|} \sum_{x \in D} \text{Loss}(W_g(x \odot \tau), y_t), \quad (1)$$

where τ represents the backdoor trigger composed of a trigger location E_t and trigger value V_t . The objective is to minimize the difference between the target label y_t and the output results of the global model W_g when taking the backdoored images as input, which can be quantified by a loss function. The symbol \odot represents an operator to embed the backdoor trigger τ into a clean image x , whose definition is further described in (2) of Section 5. To enhance generalization performance of the optimized backdoor trigger, we employ all images in the trigger training dataset D as constraints and try to find a backdoor trigger that takes effect for all of these images.

Solving the optimization problem: To solve the above optimization problem, our approach employs two separate algorithms: one for computing the trigger location E_t (see Algorithm 1), and the other for optimizing the trigger value using E_t as input (see Algorithm 2).

Compute trigger location E_t . In Algorithm 1, we select pixel locations that contain the largest absolute gradient values with respect to the backdoor objective (1) as the trigger locations.

Algorithm 1 Computation for Trigger Location

Input: W_g, D, y_t, tri_size

Output: E_t

- 1: $\forall x \in D : y_x \leftarrow W_g(x)$.
 - 2: $\mathcal{L} \leftarrow \frac{1}{|D|} \sum_{x \in D} (y_x - y_t)^2$.
 - 3: $\forall x \in D : \delta_x \leftarrow \frac{\partial \mathcal{L}}{\partial x}$.
 - 4: $\delta \leftarrow \text{abs}(\sum_{x \in D} \delta_x)$.
 - 5: $\delta_f \leftarrow$ flatten δ into a one-dimensional array.
 - 6: $S \leftarrow \text{argsort}(\delta_f)$. {Store the sorted indices (descending sort)}
 - 7: $E_t \leftarrow S[: tri_size]$. {Top tri_size indices are trigger locations}
 - 8: $E_t \leftarrow$ transform from one-dimensional indices to indices for $x \in D$.
 - 9: **return** E_t
-

Algorithm 1 takes several inputs, including the global model W_g , the trigger training dataset D , the target label y_t , and a parameter tri_size that specifies the trigger size. The trigger size tri_size determines the number of

pixel locations we will choose. The output of the Algorithm 1 is the trigger location information denoted as E_t .

Starting from line 1 and line 2, we first calculate the loss of the global model W_g in predicting clean images in dataset D as the target label y_t , where we show Mean Square Error (MSE) as an example loss function. Next, we compute the gradient of the loss with respect to each pixel in each image and store the values of gradients in each image x in δ_x (line 3). After summing up δ_x per pixel and take the absolute value of the results, we obtain an absolute gradient value matrix with the same shape as an individual image in dataset D (line 4). To better describe how we sort elements in δ by their values, we first flatten δ into a one-dimensional array δ_f (line 5), and then sort elements in this array in descending order and store the sorted indices in an array S (line 6). The top tri_size number of indices are the trigger locations of interest, but before returning these indices, we transform them from indices for a one-dimensional array to indices for a matrix of an image’s shape in dataset D (line 7, line 8).

Optimize trigger value V_t . In Algorithm 2, we optimize the values of the trigger pixels defined in E_t using a learning-based approach.

Algorithm 2 Optimization for Trigger Value

Input: $E_t, W_g, D, y_t, n_iter, \gamma$

Output: V_t

- 1: **for** $iteration \leftarrow 1$ to n_iter **do**
 - 2: $D' \leftarrow D$.
 - 3: **if** $iteration = 1$ **then**
 - 4: $V_t \leftarrow \frac{1}{|D'|} \sum_{x \in D'} x$.
 - 5: **else if** $iteration > 1$ **then**
 - 6: $\forall x \in D' : x[E_t] \leftarrow V_t[E_t]$.
 - 7: **end if**
 - 8: $\forall x \in D' : y_x \leftarrow W_g(x)$.
 - 9: $\mathcal{L} \leftarrow \frac{1}{|D'|} \sum_{x \in D'} (y_x - y_t)^2$.
 - 10: $\forall x \in D' : \delta_x \leftarrow \frac{\partial \mathcal{L}}{\partial x}$.
 - 11: $\delta \leftarrow \sum_{x \in D'} \delta_x$.
 - 12: $V_t[E_t] \leftarrow (V_t - \gamma \cdot \delta)[E_t]$.
 - 13: **end for**
 - 14: **return** V_t
-

Algorithm 2 requires the following inputs: the trigger location E_t , the global model W_g , the trigger training dataset D , and the target label y_t . Additionally, it uses two training parameters: the number of training iterations n_iter and the learning rate γ . The output produced by Algorithm 2 is the trigger value information denoted as V_t .

The first step of each iteration is making a copy dataset D' of D (line 2) so that the optimized trigger of

each iteration can always be embedded into clean data. In the first iteration, we initialize the trigger value matrix V_t by taking the mean value of all images in dataset D' along each pixel location (line 4). Then, we calculate the loss of the global model W_g in predicting images from D' as the target label y_t (line 8, 9). Next, we compute the gradients of the loss with respect to each pixel in each image in dataset D' and store the values of gradients in each image x in δ_x (line 10). The gradient matrix δ is obtained by summing up δ_x along each pixel location (line 11) (but not need to take the absolute value as Algorithm 1). After that, we use the gradient descent technique with γ as the learning rate to only update the values of pixels within the trigger location E_t (line 12) and assign those new values to the trigger value matrix V_t . For all iterations after the initial one, we consistently replace pixels within the trigger location E_t of each image with their corresponding values in the trigger value matrix V_t (line 6). The steps of line 6 and line 12 ensure that the only variables influencing the loss result are the pixels specified by E_t .

4.4 Poisoning Malicious Clients' Training Data

The last step of our attack is to poison malicious clients' local training data using the optimized trigger $\tau = (E_t, V_t)$ and its target label y_t by a certain data poison rate. The data poison rate can be specified on a scale from 0 to 1, while smaller data poison rate induces stealthier model updates, making them more difficult for defenses to detect and filter. In the following, we set the data poison rate to 0.5 for all experiments.

5 Theoretical Analysis

In this section, we delve into the reasons behind DPOT's ability to successfully bypass state-of-the-art defenses, and analyze the improvements of an optimized trigger generated by our algorithms in assisting backdoor attacks, compared to a fixed trigger.

We use a linear regression model to explain the intuition of this work. Consider a regression problem to model the relationship between a data sample and its predicted values. We define $x \in \mathcal{D}^{1 \times n}$, where \mathcal{D} is a convex subset of \mathbb{R} as a data sample, and the vector $\hat{y} \in \mathbb{R}^{1 \times m}$ as its target values. The model $\beta \in \mathbb{R}^{n \times m}$ that makes $x\beta = \hat{y}$ is what we want to solve.

For any given data x , a backdoor attack is aiming to make the model β fit both the benign data point (x, \hat{y}) and the corresponding malicious data point (x_t, y_t) . We use $y_t \in \mathbb{R}^{1 \times m}$ to represent the backdoor target values and specify that $y_t \neq \hat{y}$. $x_t \in \mathcal{D}^{1 \times n}$ is the data x em-

bedded with a trigger τ by the following operation.

$$x_t = x(I_n - E_t) + V_t E_t, \quad (2)$$

where $V_t \in \mathcal{D}^{1 \times n}$ is a vector storing the trigger τ 's value information, and $E_t \in \{0, 1\}^{n \times n}$ is a matrix identifying the trigger τ 's location information. E_t specifies the location and shape of the trigger, defined as $E_t = \text{diag}(d_1, d_2, \dots, d_n)$, $d_i \in \{0, 1\}$, where $\sum_{i=1}^n d_i = k$. Here, k defines the number of entries in the original x that we intend to alter. The abbreviation $\text{diag}(\cdot)$ stands for a diagonal matrix whose diagonal values are specified by its arguments. I_n is an $n \times n$ identity matrix.

Definition 5.1. (Benign Loss and Benign Objective) Let $x \in \mathcal{D}^{1 \times n}$ be a benign data sample, $\hat{y} \in \mathbb{R}^{1 \times m}$ be the predicted value of x , and $\beta \in \mathbb{R}^{n \times m}$ be the prediction model. The loss to evaluate the prediction accuracy of β on the benign regression is

$$L(x, \hat{y}) = \|x\beta - \hat{y}\|_2^2. \quad (3)$$

The optimization objective to solve for β for this benign task is

$$\min_{\beta} L(x, \hat{y}). \quad (4)$$

Definition 5.2. (Backdoor Loss and Backdoor Objective) Let x_t be a backdoored data sample embedded with a trigger $\tau(V_t, E_t, y_t)$. Let $\beta \in \mathbb{R}^{n \times m}$ be the prediction model. The loss to evaluate the prediction accuracy of β on the backdoor regression is

$$L(x_t, y_t) = \|x_t\beta - y_t\|_2^2. \quad (5)$$

The optimization objective to solve for β for the backdoor task that considers both benign data and backdoor data is

$$\min_{\beta} (1 - \alpha)L(x, \hat{y}) + \alpha L(x_t, y_t), 0 \leq \alpha \leq 1. \quad (6)$$

The FL global model learns backdoor information only when it integrates malicious clients' model updates that were trained for the backdoor objective. Due to the implementation of robust aggregation, backdoor attackers have to ensure their model updates have limited divergence from those trained on benign data to avoid being filtered out by defense techniques. We term this intention as the concealment objective.

To formulate the above problem, we use gradients of optimizing the benign objective (G_{bn}) and gradients of optimizing the backdoor objective (G_{bd}) with respect to a same model β to represent model updates of a benign client and a malicious client respectively. We then use cosine similarity as a metric to evaluate the difference between G_{bn} and G_{bd} , since it is a widely used metric

in the state-of-the-art defenses [6, 22, 27, 12] to filter malicious model updates.

G_{bn} and G_{bd} are computed by

$$G_{bn} = \frac{\partial L(x, \hat{y})}{\partial \beta}, \quad (7a)$$

$$G_{bd} = \frac{\partial((1 - \alpha)L(x, \hat{y}) + \alpha L(x_t, y_t))}{\partial \beta}. \quad (7b)$$

The concealment objective is

$$\max \text{CosSim}(G_{bn}, G_{bd}). \quad (8)$$

The optimization objective used in DPOT attack is

$$\min_{V_t, E_t} \| (x(I_n - E_t) + V_t E_t)\beta - y_t \|_2^2. \quad (9)$$

Proposition 5.1. *Given a model β and a data sample x with its benign predicted value \hat{y} and a backdoor predicted value y_t , the optimization of objective (9) is a guarantee of the optimization of objective (8).*

Proof. See proof in Appendix A.1. \square

Proposition 5.1 offers a theoretical justification for DPOT’s ability to prevent malicious clients’ model updates from being detected by a commonly used metric considered in state-of-the-art defenses. In Proposition A.1 and Proposition 5.2, we demonstrate that an optimized trigger ($\hat{\tau}$) generated by learning the parameters of a given model β is more conducive to achieving the concealment objective compared to a trigger (τ_f) with fixed value, shape, and location.

Proposition 5.2. *For any fixed trigger $\tau_f(V_t, E_t, y_t)$ with specified trigger value V_t , trigger location E_t , and predicted value y_t , there exists a backdoor trigger $\hat{\tau}(\hat{V}_t, \hat{E}_t, y_t)$ that has the same y_t , but optimizes the V_t and E_t with respect to a model β , which can result in a smaller or equal backdoor loss on model β compared to τ_f .*

Proof. See proof in Appendix A.3. \square

6 Experiments

6.1 Experimental Setup

Datasets and global models: We evaluated DPOT on four classification datasets with non-IID data distributions: Fashion MNIST, FEMNIST, CIFAR10, and Tiny ImageNet. Table 1 summarizes their basic information and models we used on each dataset.

Comparisons: As DPOT is exclusively a data-poisoning attack, we compared it with existing attacks where all the non-data-poisoning components were removed. To be specific, we only implemented the trigger

Table 1: Dataset description

Dataset	#class	#img	img size	Model	#params
Fashion MNIST	10	70k	28 × 28 grayscale	2 conv 3 fc	~1.5M
FEMNIST	62	33k	28 × 28 grayscale	2 conv 2 fc	~6.6M
CIFAR10	10	60k	32 × 32 color	ResNet18	~11M
Tiny ImageNet	200	100k	64 × 64 color	VGG11	~35M

embedding part introduced in existing attacks, while disregarding any model-poisoning techniques such as objective modification, alterations to training hyperparameters, or scaling up malicious model updates. This adjustment aligns with our Trusted Execution Environments assumption as outlined in the Threat Model (Section 3).

We compared DPOT with existing attacks of three categories as described below.

- **Fixed Trigger (FT).** Following recent research on backdoor attacks on FL [2, 33, 6, 1], pixel-pattern triggers are typical backdoors applied in image classification applications. A pixel-pattern trigger is a defined arrangement of pixels with specific values and shapes, used to alter digital images at a particular location within the image. In this work, we used a pixel-pattern trigger with constantly fixed features (values, shape, and location) for all comparison experiments.
- **Distributed Fixed Trigger (DFT).** Inheriting the definition of the pixel-pattern trigger, DBA [33] slices a global pixel-pattern trigger into several parts and distributes them among different malicious FL clients for poisoning data. The attacker evaluates the Attack Success Rate on the test dataset poisoned by the global pixel-pattern trigger.
- **A3FL Trigger.** A state-of-the-art attack work in FL, A3FL [37], proposed adversarially optimizing the trigger’s value using a local model that continuously unlearns the optimized trigger information. The shape and placement of the A3FL trigger stay fixed during optimization. We compare their methods on CIFAR10 dataset as it is the only available configuration in their open-source project.

The visualization of various trigger types are demonstrated in Figures 5, 6, 7, and 9.

Defenses: We evaluated backdoor attacks in FL systems employing different state-of-the-art defense strategies against backdoor attacks. We selected defense baselines based on two criteria: 1) Defenses provided accessible proof-of-concept code to ensure accurate implementation of the proposed ideas; 2) Defenses either claimed

or were proven by existing research to have defense effectiveness against backdoor attacks in FL. Detailed descriptions of these defenses were presented in Section B.

Evaluation metrics: We considered three metrics to evaluate the effectiveness and stealthiness of backdoor attacks when confronted with different defense strategies.

Final Attack Success Rate (Final *ASR*). This metric quantifies the proportion of test images poisoned with the same backdoor trigger used during training that were misclassified as the target label by the final global model. In order to reduce the testing error caused by noise on data or model so as to maintain the fairness of comparison, we tested *ASR* on the global models of the last five rounds and took their mean value as the Final *ASR*.

Average Attack Success Rate (Avg *ASR*). We start attacking from the first round of FL training. Since the attack cycle of DPOT is an individual round, we introduced Avg *ASR* to assess the average effectiveness for every round’s attack during the FL process. To evaluate *ASR* for an individual round, we poison test data with the optimized trigger $\tau^{(i)}$ which was generated using the current-round global model $W_g^{(i)}$ and test the *ASR* on the next-round global model $W_g^{(i+1)}$. We took the average of the *ASR* of all rounds in the FL process as the Avg *ASR*. The implication of a high Avg *ASR* of an attack is that this attack had consistently significant effectiveness during the whole FL process, ensuring a high Final *ASR* no matter when the FL process ended.

Main-task Accuracy (*MA*). This metric measures the stealthiness of a backdoor attack by testing the accuracy of a global model on the clean test dataset. A backdoor attack was determined to be stealthy if its victim model did not show a noticeable reduction in *MA* compared to the benign model.

FL configurations: The FEMNIST dataset [5] provides each client’s local training data with a naturally non-IID guarantee. For Fashion MNIST, CIFAR10, and Tiny ImageNet datasets, we distributed training data to FL clients using the same method introduced by FLTrust [6], where we set the non-IID bias to be 0.5.

Following the standard setup [15], we used SGD optimization with CrossEntropy loss and a mini-batch size of 256. In experiments on Tiny ImageNet, we set mini-batch size as 64. Each FL client trained a global model for $n_{epoch} = 5$ local epochs with its local data in one global round.

For training Fashion MNIST and FEMNIST datasets, we used a static local learning rate (*lr*) of 0.01. For training the larger and more complicated datasets such as CIFAR10 and Tiny ImageNet, we applied the learning rate schedule technique following the instructions in the

related machine learning works [15, 28] to boost DNN models’ performance.

Attack configurations: In our algorithm 2 for training a trigger value, we set the number of training iterations to $n_{iter} = 10$, which proved sufficient for obtaining the optimal trigger values. The learning rate γ started from 5 and was halved when the training loss increased compared to the previous iteration.

Table 2 shows the default settings of DPOT attack for experiments. In particular, we consider the following attributes that are critical for attack effectiveness.

Trigger size. We defined trigger size for different datasets according to the following three criteria. First, a trigger of the defined trigger size should not be able to cover important details of any images and lead humans to misidentify the images from their original labels. To show that we follow this criteria, we demonstrated poisoned images from different datasets that are embedded with DPOT triggers, as shown in Figure 2 and 8. Second, on basis of the first criterion, we adjust trigger size to match the image size and the feature size of different datasets. Specifically, if a dataset contains images with high resolution (large image size), then a large trigger size is needed to effectively match it (Tiny ImageNet vs. CIFAR10). If images in a dataset contain large visual elements or patterns, then a large trigger size is needed to effectively match it (Fashion MNIST vs. FEMNIST). Third, we found that when using models with deep model architectures or having large number of parameters, a small trigger size is sufficient for conducting DPOT attack (CIFAR10 vs. Fashion MNIST).

Round. We determine the number of training rounds for each dataset by measuring the convergence time on an FL pipeline using FedAvg as the aggregation rule. Convergence is considered achieved when the test accuracy on the main task stabilizes within a range of 0.5 percentage points over a period of five consecutive rounds of training.

Number of clients. The number of clients varies across different datasets due to a balance between our available computational resources and the size of the datasets/models. All clients participate in the aggregation for each round of FL training.

MCR. Malicious Client Ratio (MCR) is a parameter defining the proportion of compromised clients compared to the total number of clients in each-round aggregation. We consider 5% as the default MCR (for FL systems having 50 clients, 2 of them are malicious clients), which is smaller than the state-of-the-art attacks [37, 20, 10] that require at least 10% of clients to behave maliciously during aggregation.

Local data poison rate. It specifies the proportion of data that has been manipulated with a backdoor attack compared to the total amount of data available in

each malicious client.

Table 2: Default Settings

	Fashion MNIST	FEMNIST	CIFAR10	Tiny ImageNet
Trigger Size	64	25	25	64
Round	300	200	150	100
Number of Clients	100	100	50	50
MCR	0.05			
Local Data Poison Rate	0.5			

Experiment environment and code: We conducted all the experiments on a platform with an NVIDIA Quadro RTX 6000 Graphic Card having 24 GB GPU memory in each chip and an Intel(R) Xeon(R) Gold 6230 CPU @2.10GHz having 384 GB CPU memory. We implemented all the algorithms using the PyTorch framework. We will open-source this project after its publication.

6.2 Experimental Results

6.2.1 Representative Results

In this section, we presented the performance of DPOT attack under nine defense methods and compared our results with two widely-used data-poisoning attacks.

The effectiveness of an attack is measured using the *ASR* metric, as shown in Figure 3. Results indicate that the DPOT attack consistently achieves a final *ASR* exceeding 50% across all considered defense methods, regardless of the dataset’s characteristics such as size and number of images. Additionally, the DPOT attack also exhibits a considerable average *ASR* in each attack practice, indicating its malicious effect on each-round global model. The stealthiness of an attack is assessed using the *MA* metric, as indicated in Table 3. We established a baseline *MA* for each defense method on every dataset by measuring the final *MA* achieved in an attack-free FL training session employing the respective defense. Upon comparing the baseline *MA* of various defenses to that of FedAvg, we observed that certain defenses, such as Krum on every dataset and FLAME on Tiny ImageNet, failed to achieve similar convergence performance as FedAvg under the same training conditions. Defenses with deficient baseline *MA* are less likely to be adopted in practice, and experimental results obtained using these defenses are not generally representative. The results presented in Table 3 indicate that the DPOT attack successfully maintains the *MA* of victim global models within a ± 2 percentage-point difference range compared to the corresponding baseline *MA* values.

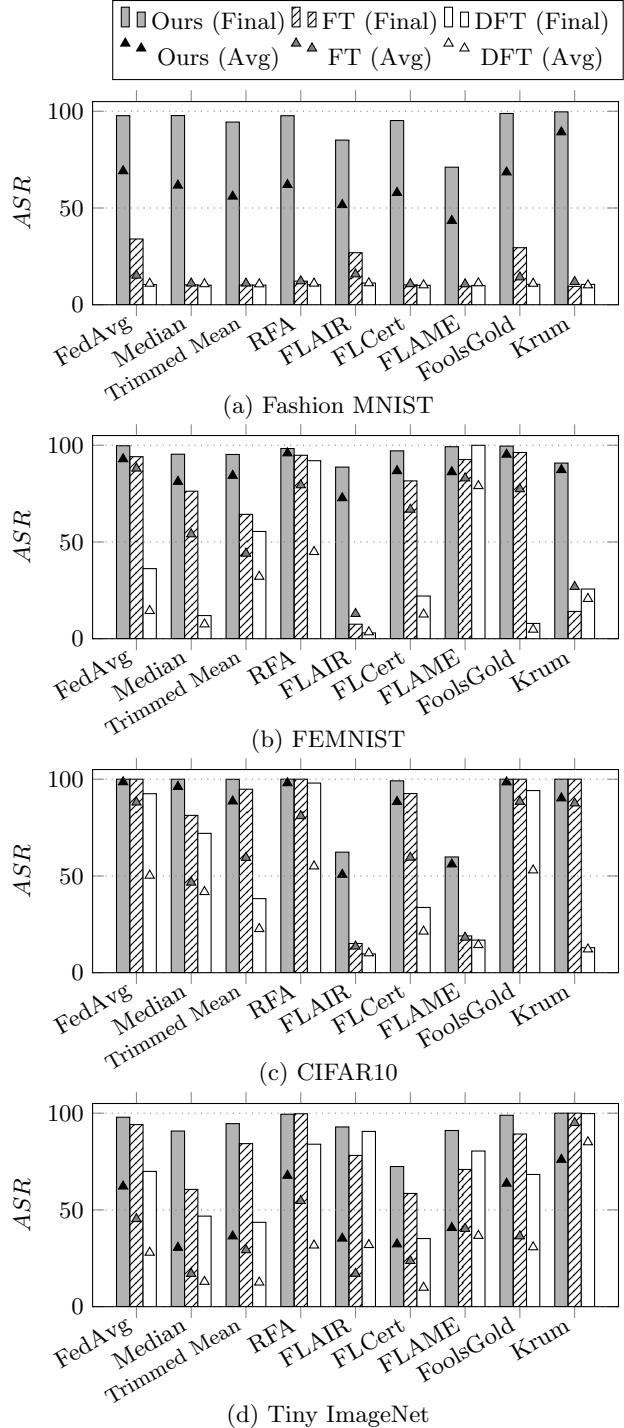


Figure 3: Representative results on four different datasets are provided. The attack settings correspond to the default settings outlined in Table 2.

In comparison to FT and DFT attacks, the DPOT attack demonstrates superior attack effectiveness in compromising existing defenses. As illustrated in Figure 3, the DPOT attack consistently exhibits higher *ASR*, both in the final and average metrics, compared to FT and

MA	Tiny ImageNet				Fashion MNIST				FEMNIST				CIFAR10			
	None	Ours	FT	DFT	None	Ours	FT	DFT	None	Ours	FT	DFT	None	Ours	FT	DFT
FedAvg	43.9	43.5	43.0	43.3	86.7	87.3	86.7	86.8	82.2	81.4	83.3	82.3	70.3	70.7	70.4	71.4
Median	40.6	40.2	40.6	38.6	86.0	85.8	86.6	86.3	80.4	81.5	79.8	79.9	70.2	69.1	69.8	69.7
Trimmed Mean	40.8	40.4	40.1	40.6	86.4	85.8	86.4	86.3	80.2	81.7	81.3	81.2	69.4	70.4	70.2	70.8
RFA	43.6	43.0	43.0	43.0	86.4	86.0	87.1	87.1	83.0	80.7	81.0	80.8	70.4	70.7	70.3	70.8
FLAIR	43.6	42.6	41.8	42.1	86.1	84.9	85.2	84.4	81.5	80.7	80.6	79.7	70.3	70.6	71.0	70.4
FLCert	40.3	40.2	39.7	39.7	86.2	85.9	86.0	86.8	81.3	80.9	81.5	81.0	69.6	70.0	69.8	70.4
FLAME	29.9	28.7	29.2	28.9	86.4	86.4	86.4	86.7	81.8	80.2	80.7	81.0	70.1	70.3	70.9	70.9
FoolsGold	43.1	43.2	43.5	43.2	86.6	87.1	86.8	87.3	83.4	82.7	83.0	81.8	70.4	71.0	71.2	71.7
Krum	17.7	10.9	0.5	8.0	81.6	76.8	81.3	81.1	71.5	72.0	71.8	71.9	47.2	41.9	35.9	49.7

Table 3: Main-task Accuracy (MA) for representative results. "None" represents no attack existing in the FL training.

DFT attacks. The only exception is Krum on Tiny ImageNet, where the FL training failed to converge with any attacks (refer to Table 3).

6.2.2 Comparison to A3FL Trigger

We compared the performance of DPOT attack with the A3FL [37] attack. We implemented the A3FL attack by faithfully replicating the attacker’s actions as designed by A3FL, with reference to their open-source code. This was done while considering the attacking scenario aligned with our FL configurations and attack settings (refer to Table 2).

The results in Table 4 demonstrate that our attack achieved significantly higher *ASR* values in both the final and average metrics compared to the A3FL attack, except for the one employing Krum as the aggregation rule, which failed to converge. This suggests that the optimized triggers generated using our algorithms are more effective in compromising FL global models through data poisoning compared to those generated using A3FL’s techniques. Additionally, we observed that the *ASR* results of A3FL were even worse than those of FT and DFT (as shown in Figure 3). This implies that dynamically changing the backdoor objective may not always enhance the effectiveness of backdoor attacks compared to maintaining a static backdoor objective. Therefore, it is always essential to consider whether the modified backdoor objective can truly accelerate the learning of backdoor information by global models and if the process of constructing the new backdoor objective has been sufficiently developed.

6.2.3 Analysis of the DPOT working principles

In this section, we analyze the attack effectiveness of each component of the DPOT attack’s working principles and report evidence that it effectively conceals malicious clients’ model updates, thereby integrating them into the global models through aggregation.

In the i -th round, DPOT generates a trigger $\tau^{(i)}$ by optimizing its shape, location and values to make the

	Final <i>ASR</i>		Avg <i>ASR</i>		MA	
	Ours	A3FL	Ours	A3FL	Ours	A3FL
FedAvg	100	48.9	98.5	38.1	70.7	70.6
Median	100	32.9	96.1	24.0	69.1	69.1
Trimmed Mean	100	35.0	88.6	23.5	70.4	69.9
RFA	100	24.7	97.8	23.8	70.7	70.2
FLAIR	62.3	13.2	50.7	12.5	70.6	70.7
FLCert	99.2	39.0	88.3	28.4	70.0	69.9
FLAME	59.8	13.7	56.0	32.1	70.3	70.1
FoolsGold	100	46.9	98.5	38.0	71.0	70.8
Krum	100	99.9	90.2	92.4	41.9	38.0

Table 4: Comparison results with A3FL attack on CIFAR10.

global model of this round $W_g^{(i)}$ achieve a maximum *ASR*. However, what we are truly interested in is the *ASR* on the global model after the i -th round aggregation, which is the next-round global model denoted as $W_g^{(i+1)}$. The attack effectiveness of the trigger $\tau^{(i)}$ on the global model $W_g^{(i+1)}$ stems from two reasons:

1. **Trigger Optimization:** Trigger optimization using $W_g^{(i)}$ results in the improvement of the *ASR* on $W_g^{(i+1)}$.
2. **Concealment of Model Updates:** Malicious training data partially poisoned by $\tau^{(i)}$ results in trivial differences in model updates compared to benign training data, enabling them to be aggregated into $W_g^{(i+1)}$, thereby making $W_g^{(i+1)}$ learn the backdoor information introduced by $\tau^{(i)}$.

In the following, we explain how we designed experiments to study the impact of each reason, and analyzed the experiment results.

Experiment design: To assess the attack effectiveness brought by Trigger Optimization, we eliminated any effects produced by data poisoning. Specifically, we set all clients in the FL system to be benign, ensuring that the next-round global model, denoted as $\widetilde{W}_g^{(i+1)}$, aggregates benign model updates only. In the meantime, we still collected data from a certain number of clients

and optimized a trigger $\tilde{\tau}^{(i)}$ for $\widetilde{W}_g^{(i)}$. Then, we tested $\widetilde{W}_g^{(i+1)}$ on a dataset in which all images are poisoned with the trigger $\tilde{\tau}^{(i)}$ to obtain an \widetilde{ASR} . This \widetilde{ASR} evaluates the attack effectiveness achieved by the current-round optimized trigger $\tau^{(i)}$ on the next-round global model $\widetilde{W}_g^{(i+1)}$, which does not contain any model updates learned from backdoor information.

To assess the attack effectiveness brought by Concealment of Model Updates, we introduced malicious clients into the FL system and therefore the global model, denoted as $\ddot{W}_g^{(i+1)}$, was allowed to aggregate model updates submitted by malicious clients. In this system, malicious clients partially poisoned their local training data (aligning with default settings in Table 2) using the trigger $\tilde{\tau}^{(i)}$ that was optimized for $\widetilde{W}_g^{(i)}$, and then conducted their local training. We tested the $\ddot{W}_g^{(i+1)}$ on the testing dataset that was also poisoned by $\tilde{\tau}^{(i)}$ to obtain an $A\ddot{S}R$. We evaluated the attack effectiveness of Concealment of Model Updates by measuring the increase in ASR compared to the previous setting, calculated as $(A\ddot{S}R - \widetilde{ASR})$. This metric reveals how much the malicious clients’ model updates influenced the global model $\ddot{W}_g^{(i+1)}$ to achieve a higher ASR compared to $\widetilde{W}_g^{(i+1)}$.

	ASR type	Fashion MNIST		FEMNIST		CIFAR10	
		Final	Avg	Final	Avg	Final	Avg
FedAvg	\widetilde{ASR}	58.8	45.1	54.0	28.6	55.6	50.9
	$A\ddot{S}R$	97.7	69.1	99.7	92.9	100	98.5
Median	\widetilde{ASR}	57.9	38.2	18.0	17.5	56.6	48.7
	$A\ddot{S}R$	97.8	61.7	95.4	81.2	100	96.1
Trimmed Mean	\widetilde{ASR}	31.6	29.7	24.2	25.6	55.6	40.9
	$A\ddot{S}R$	94.4	56.0	95.2	84.3	100	88.6
RFA	\widetilde{ASR}	78.0	46.4	18.9	13.4	57.4	46.1
	$A\ddot{S}R$	97.7	62.0	98.3	95.9	100.0	97.8
FLAIR	\widetilde{ASR}	42.2	36.2	23.0	29.6	54.1	45.9
	$A\ddot{S}R$	85.3	50.1	88.7	72.7	62.3	50.7
FLCert	\widetilde{ASR}	49.6	39.7	27.7	34.6	48.7	46.7
	$A\ddot{S}R$	95.2	57.9	97.1	86.7	99.2	88.3
FLAME	\widetilde{ASR}	38.0	26.2	34.7	35.7	28.1	51.0
	$A\ddot{S}R$	71.1	43.4	99.2	86.1	59.8	56.1
Fools Gold	\widetilde{ASR}	54.2	50.3	57.0	43.7	35.5	35.6
	$A\ddot{S}R$	98.9	68.5	99.6	95.2	100	98.5
Krum	\widetilde{ASR}	62.3	42.9	50.9	31.3	20.7	24.0
	$A\ddot{S}R$	99.7	89.2	90.8	87.2	100	90.2

Table 5: ASR under different attacking conditions. \widetilde{ASR} assesses the attack effectiveness of “Trigger Optimization” alone, while $A\ddot{S}R$ assesses the combined effectiveness of both “Trigger Optimization” and “Concealment of Model Updates”.

Experiment results: Table 5 shows results of \widetilde{ASR} and $A\ddot{S}R$ over 9 different defense methods. We used same settings as in Table 2 for testing $A\ddot{S}R$, and kept the size of trigger training dataset consistent when testing \widetilde{ASR} .

The results of \widetilde{ASR} in Table 5 show that different defense methods resulted in very different \widetilde{ASR} even for the same learning task of a dataset. The reason for the variance of \widetilde{ASR} is the gap between $W_g^{(i)}$ and $\widetilde{W}_g^{(i+1)}$ were different when implementing different defense methods. If the gap between consecutive rounds of global models in an FL system is smaller, Trigger Optimization will be more effective in its attack [20, 37].

The results of $A\ddot{S}R$ in Table 5 show that the presence of malicious clients’ model updates consistently enhances ASR compared to \widetilde{ASR} across all defense methods on different datasets. We consider this enhancement as an evidence of the statement that the attack effectiveness of DPOT comes from both Trigger Optimization and Concealment of Model Updates, with the latter one playing a critical role in producing a high $A\ddot{S}R$.

A general hypothesis made by the state-of-the-art defenses against backdoor attacks in FL is that malicious clients’ model updates have a distinct divergence from benign clients’ model updates. However, as indicated by the results in Table 5, DPOT effectively conceals the model updates from malicious clients amidst those of benign clients, eluding detection and filtering by state-of-the-art defenses. Consequently, defenses formulated based on this broad hypothesis inherently face limitations when challenged by DPOT attacks.

6.2.4 Impact of Malicious Client Ratio (MCR)

In this section, we evaluated the impact of different Malicious Client Ratios (MCR) on the performance of DPOT attack. We assumed that the number of malicious clients in the FL system should be kept small ($\leq 30\%$) for practical reasons. We varied the MCR across four different settings (0.05, 0.1, 0.2, and 0.3) while keeping other settings consistent with those in Table 2. We experimented over nine different defenses on the learning tasks of the CIFAR10 datasets and compare DPOT’s results with FT and DFT.

Tables 6 presents the evaluation results of attack effectiveness. DPOT exhibited a dominant advantage over FT and DFT when the MCR is small (0.05 and 0.1). However, this advantage diminished with increasing MCR, indicating that when a sufficient number of malicious clients present in FL, even FT and DFT can achieve respectable ASR against certain defense strategies. In most cases, the ASR for all attacks continued to rise as the MCR increased, with the exception of FLAME. Results obtained with FLAME indicate that

MCR	Final <i>ASR</i>												Average <i>ASR</i>											
	0.05			0.1			0.2			0.3			0.05			0.1			0.2			0.3		
	Ours	FT	DFT	Ours	FT	DFT	Ours	FT	DFT	Ours	FT	DFT	Ours	FT	DFT	Ours	FT	DFT	Ours	FT	DFT	Ours	FT	DFT
FedAvg	100	100	100	100	100	100	100	100	100	100	100	100	99	88	50	99	96	88	99	99	92	99	100	97
Median	100	81	72	100	100	97	100	100	100	100	100	100	96	47	42	97	79	63	99	97	82	99	98	93
Trimmed Mean	100	95	38	100	100	99	100	100	100	100	100	100	89	59	23	98	82	69	99	94	85	99	99	92
RFA	100	100	98	100	100	100	100	100	100	100	100	100	98	81	55	99	95	90	99	99	97	99	99	98
FLAIR	62	15	10	58	25	9	67	27	22	82	33	40	51	14	10	64	24	9	68	24	16	84	42	30
FLCert	99	93	34	100	100	95	100	100	100	100	100	100	88	60	21	98	87	60	98	94	83	99	99	91
FLAME	60	19	17	52	18	51	50	16	16	55	19	16	56	18	14	66	19	34	53	19	16	70	23	43
FoolsGold	100	100	94	100	100	100	100	100	100	100	100	100	98	88	53	99	97	87	99	99	95	99	99	98
Krum	100	100	13	100	100	100	100	84	100	100	95	100	90	88	12	97	98	84	99	94	92	99	100	97

Table 6: The effects of malicious client ratio on the effectiveness of different attacks (CIFAR10).

the number of malicious clients did not significantly impact its defense effectiveness.

Table 8 presents the Main-task Accuracy results for each experiment considered in this section. Except for experiments applying Krum as the aggregation rule, all MA results for different attacks remain similar to the baseline MA, indicating the correct implementation of each attack.

6.2.5 Impact of Trigger Size

Trigger Size, determining how many pixels in an image we can alter, is an important parameter for DPOT attack. Larger trigger size generally results in a better optimization performance. However, it is essential to strike a balance because an excessively large trigger size will make a trigger obscure important details of images, making the trigger easier to perceive by humans. In this section, we assessed the impact of different trigger sizes on the performance of different attacks. We explored trigger sizes across four different settings (9, 25, 49, and 100) while maintaining other settings in accordance with those outlined in Table 2. We demonstrated experiment results involving nine different defense strategies on the CIFAR10 datasets and compared the results achieved by DPOT with those of FT and DFT.

Tables 7 shows that DPOT maintained a significant advantage in *ASR* over FT and DFT across various trigger sizes, ranging from small to large. According to the results, we found that FT and DFT did not benefit from larger trigger sizes in achieving higher *ASR* when encountering with robust aggregations that have advanced defense effectiveness, such as FLAIR and FLAME. A possible explanation on that is when malicious model updates were trained on data poisoned with larger FT or DFT triggers, they exhibited greater divergence from benign model updates, making them more susceptible to detection and filtering by defense mechanisms. In contrast, DPOT demonstrated a continuous improvement in *ASR* as the trigger size increased.

Table 9 presents the Main-task Accuracy results for

each experiment considered in this section. Results in it indicate correctness in our implementation.

6.2.6 Effects of the scaling-based model poisoning techniques

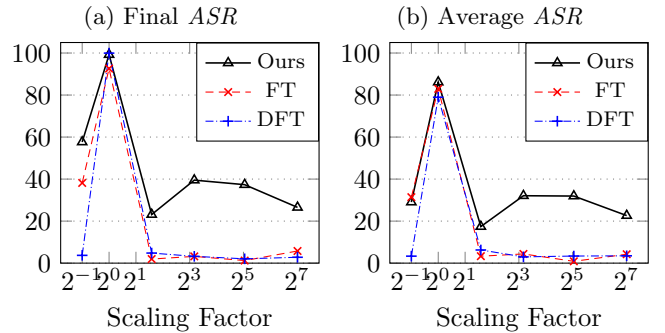


Figure 4: Comparison results of different attacks when employing the scaling-based model poisoning technique to undermine FLAME defense (implemented on the FEMNIST dataset).

In this section, we removed the TEEs assumption and conducted experiments to examine the effects of employing scaling-based model poisoning techniques on the attack performance of DPOT, FT, and DFT. By incorporating the model poisoning technique, our implementation of FT and DFT pipelines aligns more closely with the attack strategies introduced in state-of-the-art backdoor attacks on FL [1, 33].

Our experiments were designed within an FL system utilizing FLAME as its aggregation rule and FEMNIST dataset as its main training task. We adjusted the scaling factors, used to scale malicious clients’ model updates, to be 0.5, 1, 3, 9, 33, and 129 respectively. Figures 4a and 4b illustrate the results of Final *ASR* and Avg *ASR* of various attacks in response to different scaling factors.

We observed that when the scaling factor is 1, all DPOT, FT, and DFT pipelines exhibit comparable and high *ASR* against FLAME defense. However, as the scaling factor increases, FLAME demonstrates robust

Trigger Size	Final ASR												Average ASR											
	9			25			49			100			9			25			49			100		
	Ours	FT	DFT	Ours	FT	DFT	Ours	FT	DFT	Ours	FT	DFT	Ours	FT	DFT	Ours	FT	DFT	Ours	FT	DFT	Ours	FT	DFT
FedAvg	100	94	49	100	100	93	100	100	91	100	100	77	95	60	28	99	88	50	99	90	59	99	93	52
Median	97	23	12	100	81	72	100	95	25	100	99	46	66	21	12	96	47	42	98	66	17	99	82	29
Trimmed Mean	98	51	14	100	95	38	100	99	43	100	100	74	71	29	13	89	59	23	99	74	27	99	79	44
RFA	100	100	99	100	100	98	100	100	100	100	100	98	93	79	56	98	81	55	99	81	71	99	90	73
FLAIR	27	14	14	62	15	10	89	22	15	99	24	14	24	14	13	51	14	10	84	22	15	98	16	13
FLCert	99	38	14	99	93	34	100	88	51	100	100	49	78	26	13	88	60	21	99	59	23	99	78	33
FLAME	21	18	12	60	19	17	100	12	11	100	33	31	35	17	12	56	18	14	84	17	11	90	31	24
FoolsGold	100	100	43	100	100	94	100	100	98	100	100	81	93	72	23	98	88	53	99	94	69	99	94	55
Krum	100	100	99	100	100	13	100	100	100	100	100	100	98	92	62	90	88	12	98	97	83	99	99	83

Table 7: The effects of trigger size on the effectiveness of different attacks (CIFAR10).

defense performance, significantly reducing the *ASR* of every attack pipeline. Despite this mitigation, DPOT shows greater resilience in attack effectiveness compared to FT and DFT. The optimized trigger generated by our algorithms retains intrinsic attack effects on the global model even without successful data-poisoning techniques. When the scaling factor is reduced to 0.5, malicious model updates are expected to be stealthier, yet their contributions to the aggregated global model are also mitigated, resulting in reduced *ASR* for all attack pipelines compared to when the scaling factor is 1.

7 Conclusion and Future Work

In this work, we proposed DPOT, a novel backdoor attack method in federated learning (FL). DPOT dynamically adjusts the backdoor objective to conceal malicious clients’ model updates among benign ones, enabling global models to aggregate them even when protected by state-of-the-art defenses. DPOT attack is easy to implement, relying solely on data poisoning, yet it poses a significant threat to existing defense methods and causes a usability detriment to the FL global model.

Interesting future works based on this paper’s contributions involve three directions: 1) Explore whether similar vulnerabilities exist in other machine learning scenarios. For example, in the training scenario of foundation models where agents of a domain want to collaboratively train a downstream model without sharing their private data, this distributed and privacy-preserved learning system might also be vulnerable to attacks similar to DPOT. Additionally, in the training scenario of Vertical FL, it is intriguing to investigate if attacks can have similar effects like DPOT. 2) Extension to different learning tasks. In this work, we only discuss one learning task, which is image classification. It would be interesting to develop similar attacks for other learning tasks trained on different distributions, such as language generation tasks. 3) Defense against DPOT attacks. As we showed that model updates, gradients,

and neuron behaviors might not be good features to use in analyzing abnormal submissions from clients, more diverse defense techniques are called for to mitigate our attacks.

References

- [1] Eugene Bagdasaryan, Andreas Veit, Yiqing Hua, Deborah Estrin, and Vitaly Shmatikov. 2020. How to backdoor federated learning. In *International Conference on Artificial Intelligence and Statistics*. PMLR, 2938–2948.
- [2] Gilad Baruch, Moran Baruch, and Yoav Goldberg. 2019. A little is enough: Circumventing defenses for distributed learning. *Advances in Neural Information Processing Systems* 32 (2019).
- [3] Arjun Nitin Bhagoji, Supriyo Chakraborty, Prateek Mittal, and Seraphin Calo. 2019. Analyzing federated learning through an adversarial lens. In *International Conference on Machine Learning*. PMLR, 634–643.
- [4] Peva Blanchard, El Mahdi El Mhamdi, Rachid Guerraoui, and Julien Stainer. 2017. Machine learning with adversaries: Byzantine tolerant gradient descent. *Advances in neural information processing systems* 30 (2017).
- [5] Sebastian Caldas, Sai Meher Karthik Duddu, Peter Wu, Tian Li, Jakub Konečný, H Brendan McMahan, Virginia Smith, and Ameet Talwalkar. 2018. Leaf: A benchmark for federated settings. *arXiv preprint arXiv:1812.01097* (2018).
- [6] Xiaoyu Cao, Minghong Fang, Jia Liu, and Neil Zhenqiang Gong. 2020. Fltrust: Byzantine-robust federated learning via trust bootstrapping. *arXiv preprint arXiv:2012.13995* (2020).
- [7] Xiaoyu Cao, Zaixi Zhang, Jinyuan Jia, and Neil Zhenqiang Gong. 2022. Flocert: Provably secure federated learning against poisoning attacks.

IEEE Transactions on Information Forensics and Security 17 (2022), 3691–3705.

- [8] Xinyun Chen, Chang Liu, Bo Li, Kimberly Lu, and Dawn Song. 2017. Targeted backdoor attacks on deep learning systems using data poisoning. *arXiv preprint arXiv:1712.05526* (2017).
- [9] Minghong Fang, Xiaoyu Cao, Jinyuan Jia, and Neil Gong. 2020. Local model poisoning attacks to {Byzantine-Robust} federated learning. In *29th USENIX security symposium (USENIX Security 20)*. 1605–1622.
- [10] Pei Fang and Jinghui Chen. 2023. On the vulnerability of backdoor defenses for federated learning. In *Proceedings of the AAAI Conference on Artificial Intelligence*, Vol. 37. 11800–11808.
- [11] Clement Fung, Chris JM Yoon, and Ivan Beschastnikh. 2018. Mitigating sybils in federated learning poisoning. *arXiv preprint arXiv:1808.04866* (2018).
- [12] Clement Fung, Chris J. M. Yoon, and Ivan Beschastnikh. 2020. The Limitations of Federated Learning in Sybil Settings. In *23rd International Symposium on Research in Attacks, Intrusions and Defenses (RAID 2020)*. USENIX Association, San Sebastian, 301–316. <https://www.usenix.org/conference/raid2020/presentation/fung>
- [13] Xueluan Gong, Yanjiao Chen, Huayang Huang, Yuqing Liao, Shuai Wang, and Qian Wang. 2022. Coordinated backdoor attacks against federated learning with model-dependent triggers. *IEEE network* 36, 1 (2022), 84–90.
- [14] Tianyu Gu, Kang Liu, Brendan Dolan-Gavitt, and Siddharth Garg. 2019. Badnets: Evaluating backdooring attacks on deep neural networks. *IEEE Access* 7 (2019), 47230–47244.
- [15] Kaiming He, Xiangyu Zhang, Shaoqing Ren, and Jian Sun. 2016. Deep residual learning for image recognition. In *Proceedings of the IEEE conference on computer vision and pattern recognition*. 770–778.
- [16] Soheil Kolouri, Aniruddha Saha, Hamed Pirsiavash, and Heiko Hoffmann. 2020. Universal litmus patterns: Revealing backdoor attacks in cnns. In *Proceedings of the IEEE/CVF Conference on Computer Vision and Pattern Recognition*. 301–310.
- [17] K. Kumari, P. Rieger, H. Fereidooni, M. Jadliwala, and A. Sadeghi. 2023. BayBFed: Bayesian Backdoor Defense for Federated Learning. In *2023 2023 IEEE Symposium on Security and Privacy (SP) (SP)*.
- [18] Junyu Lin, Lei Xu, Yingqi Liu, and Xiangyu Zhang. 2020. Composite backdoor attack for deep neural network by mixing existing benign features. In *Proceedings of the 2020 ACM SIGSAC Conference on Computer and Communications Security*. 113–131.
- [19] Yingqi Liu, Shiqing Ma, Yousra Aafer, Wen-Chuan Lee, Juan Zhai, Weihang Wang, and Xiangyu Zhang. 2018. Trojaning attack on neural networks. In *25th Annual Network And Distributed System Security Symposium (NDSS 2018)*. Internet Soc.
- [20] Xiaoting Lyu, Yufei Han, Wei Wang, Jingkai Liu, Bin Wang, Jiqiang Liu, and Xiangliang Zhang. 2023. Poisoning with Cerberus: Stealthy and Colluded Backdoor Attack against Federated Learning. *Proceedings of the AAAI Conference on Artificial Intelligence* 37 (Jun. 2023), 9020–9028.
- [21] Brendan McMahan, Eider Moore, Daniel Ramage, Seth Hampson, and Blaise Aguerre y Arcas. 2017. Communication-efficient learning of deep networks from decentralized data. In *Artificial intelligence and statistics*. PMLR, 1273–1282.
- [22] Thien Duc Nguyen, Phillip Rieger, Roberta De Viti, Huili Chen, Björn B Brandenburg, Hossein Yalame, Helen Möllering, Hossein Fereidooni, Samuel Marchal, Markus Miettinen, et al. 2022. {FLAME}: Taming backdoors in federated learning. In *31st USENIX Security Symposium (USENIX Security 22)*. 1415–1432.
- [23] Krishna Pillutla, Sham M. Kakade, and Zaid Harchaoui. 2022. Robust Aggregation for Federated Learning. *IEEE Transactions on Signal Processing* 70 (2022), 1142–1154. <https://doi.org/10.1109/TSP.2022.3153135>
- [24] Phillip Rieger, Torsten Krauß, Markus Miettinen, Alexandra Dmitrienko, and Ahmad-Reza Sadeghi. 2022. Crowdguard: Federated backdoor detection in federated learning. *arXiv preprint arXiv:2210.07714* (2022).
- [25] Moritz Schneider, Ramya Jayaram Masti, Shweta Shinde, Srdjan Capkun, and Ronald Perez. 2022. SoK: Hardware-supported trusted execution environments. *arXiv preprint arXiv:2205.12742* (2022).
- [26] Ali Shafahi, W Ronny Huang, Mahyar Najibi, Octavian Suci, Christoph Studer, Tudor Dumitras, and Tom Goldstein. 2018. Poison frogs! targeted

- clean-label poisoning attacks on neural networks. *Advances in neural information processing systems* 31 (2018).
- [27] Atul Sharma, Wei Chen, Joshua Zhao, Qiang Qiu, Saurabh Bagchi, and Somali Chaterji. 2023. FLAIR: Defense against Model Poisoning Attack in Federated Learning. In *ASIA CCS '23*. Association for Computing Machinery.
- [28] Karen Simonyan and Andrew Zisserman. 2014. Very deep convolutional networks for large-scale image recognition. *arXiv preprint arXiv:1409.1556* (2014).
- [29] Ziteng Sun, Peter Kairouz, Ananda Theertha Suresh, and H Brendan McMahan. 2019. Can you really backdoor federated learning? *arXiv preprint arXiv:1911.07963* (2019).
- [30] Bolun Wang, Yuanshun Yao, Shawn Shan, Huiying Li, Bimal Viswanath, Haitao Zheng, and Ben Y Zhao. 2019. Neural cleanse: Identifying and mitigating backdoor attacks in neural networks. In *2019 IEEE Symposium on Security and Privacy (SP)*. IEEE, 707–723.
- [31] Hongyi Wang, Kartik Sreenivasan, Shashank Rajput, Harit Vishwakarma, Saurabh Agarwal, Jy-yong Sohn, Kangwook Lee, and Dimitris Papailiopoulos. 2020. Attack of the Tails: Yes, You Really Can Backdoor Federated Learning. In *Proceedings of the 34th International Conference on Neural Information Processing Systems (NIPS'20)*. Article 1348, 15 pages.
- [32] Kang Wei, Jun Li, Chuan Ma, Ming Ding, Sha Wei, Fan Wu, Guihai Chen, and Thilina Ranbaduge. 2022. Vertical federated learning: Challenges, methodologies and experiments. *arXiv preprint arXiv:2202.04309* (2022).
- [33] Chulin Xie, Keli Huang, Pin-Yu Chen, and Bo Li. 2020. DBA: Distributed Backdoor Attacks against Federated Learning. In *International Conference on Learning Representations*. <https://openreview.net/forum?id=rkgyS0VFvr>
- [34] Kan Xie, Zhe Zhang, Bo Li, Jiawen Kang, Dusit Niyato, Shengli Xie, and Yi Wu. 2022. Efficient federated learning with spike neural networks for traffic sign recognition. *IEEE Transactions on Vehicular Technology* 71, 9 (2022), 9980–9992.
- [35] Yuanshun Yao, Huiying Li, Haitao Zheng, and Ben Y Zhao. 2019. Latent backdoor attacks on deep neural networks. In *Proceedings of the 2019 ACM SIGSAC conference on computer and communications security*. 2041–2055.
- [36] Dong Yin, Yudong Chen, Ramchandran Kannan, and Peter Bartlett. 2018. Byzantine-robust distributed learning: Towards optimal statistical rates. In *International Conference on Machine Learning*. PMLR, 5650–5659.
- [37] Hangfan Zhang, Jinyuan Jia, Jinghui Chen, Lu Lin, and Dinghao Wu. 2024. A3fl: Adversarially adaptive backdoor attacks to federated learning. *Advances in Neural Information Processing Systems* 36 (2024).
- [38] Zhengming Zhang, Ashwinee Panda, Linyue Song, Yaoqing Yang, Michael Mahoney, Prateek Mittal, Ramchandran Kannan, and Joseph Gonzalez. 2022. Neurotoxin: Durable backdoors in federated learning. In *International Conference on Machine Learning*. PMLR, 26429–26446.

A Proofs

A.1 Proof of Proposition 5.1

Proof. The gradient of benign loss (3) with respect to β is

$$g_{bn} = \frac{\partial L(x, \hat{y})}{\partial \beta} = 2x^T(x\beta - \hat{y}).$$

The gradient of backdoor loss (5) with respect to β is

$$g_{bd} = \frac{\partial L(x_t, y_t)}{\partial \beta} = 2x_t^T(x_t\beta - y_t)$$

Gradients G_{bn} and G_{bd} defined by (7a) and (7b) can be written as

$$\begin{aligned} G_{bn} &= g_{bn}. \\ G_{bd} &= (1 - \alpha)g_{bn} + \alpha g_{bd}. \end{aligned}$$

The cosine similarity between G_{bn} and G_{bd} is

$$\begin{aligned} \text{CosSim}(G_{bn}, G_{bd}) &= \frac{g_{bn} \cdot ((1 - \alpha)g_{bn} + \alpha g_{bd})}{|g_{bn}| \cdot |(1 - \alpha)g_{bn} + \alpha g_{bd}|} \\ &= \frac{g_{bn} \cdot (g_{bn} + \frac{\alpha}{1 - \alpha}g_{bd})}{|g_{bn}| \cdot |g_{bn} + \frac{\alpha}{1 - \alpha}g_{bd}|} \end{aligned}$$

One sufficiency to maximize $\text{CosSim}(G_{bn}, G_{bd})$ is to minimize the distance between g_{bn} and $g_{bn} + \frac{\alpha}{1 - \alpha}g_{bd}$, which is

$$\begin{aligned} \Delta d &= |g_{bn} - (g_{bn} + \frac{\alpha}{1 - \alpha}g_{bd})| \\ &= \frac{\alpha}{1 - \alpha} |g_{bd}|. \end{aligned}$$

Since α is a constant, minimizing Δd is equivalent to minimizing $|g_{bd}|$, which is bounded by

$$0 \leq |g_{bd}| = |2x_t^T(x_t\beta - y_t)| \leq 2 |e^T| \cdot |x_t\beta - y_t|,$$

where $e^T \in \mathbb{R}^{1 \times n}$ consists of the largest edge of the domain of x_t , e.g. $\mathbf{1}^T$ if considering normalization.

Thus, the optimization objective is to decrease $|g_{bd}|$ by minimizing its upper bound.

$$\min |x_t\beta - y_t|,$$

which can be achieved by

$$\min_{V_t, \hat{E}_t} \| (x(I_n - E_t) + V_t E_t)\beta - y_t \|_2^2.$$

□

A.2 Proposition A.1

Proposition A.1. *For any fixed trigger $\tau_f(V_t, E_t, y_t)$ with specified trigger value V_t , trigger location E_t , and predicted value y_t , there exists an optimal backdoor trigger $\hat{\tau}(\hat{V}_t, E_t, y_t)$ that has the same E_t and y_t but optimizes its V_t with respect to a model β , which can result in a smaller or equal backdoor loss on model β compared to τ_f .*

Proof. With a specified location E_t and predicted value y_t , the optimization objective for minimizing backdoor loss is

$$f = \min_{V_t} \| (x(I_n - E_t) + V_t E_t)\beta - y_t \|_2^2$$

Since $V_t \in \mathcal{D}^{1 \times n}$ where \mathcal{D} is a convex domain and $\frac{\partial^2 f}{\partial V_t^2} \succeq 0$ for any $V_t \in \mathcal{D}^{1 \times n}$, $f : \mathcal{D}^{1 \times n} \rightarrow \mathbb{R}$ is a convex function. Thus, there exists an optimal value \hat{V}_t for the objective function f in the domain $\mathcal{D}^{1 \times n}$. □

A.3 Proof of Proposition 5.2

Proof. Assume the value of data x before embedding a trigger is $[x_1, x_2, \dots, x_n]$. If an entry location in x is able to reduce the backdoor loss of β by optimizing its entry value more effectively than any individual entry location within E_t , we incorporate this location into \hat{E}_t . After constructing a \hat{E}_t , we optimize value of entries within \hat{E}_t to obtain the optimized trigger $\hat{\tau}$. We are going to prove that constructing the trigger location \hat{E}_t in this way results in the optimized trigger $\hat{\tau}$ always outperforming the fixed trigger τ_f in terms of backdoor loss.

We use k to represent the number of trigger entries that have been embedded into x . Assume the trigger value V_t is composed of $[v_1, v_2, \dots, v_n]$.

When $k = 0$, the backdoor loss is

$$L(x, y_t)_{k=0} = \|x\beta - y_t\|_2^2.$$

When $k = 1$, we calculate a location of interest i by taking the largest absolute gradient of the $L(x, y_t)_{k=0}$ with respect to all entry locations in x ,

$$i = \arg \max | \frac{\partial L(x, y_t)_{k=0}}{\partial x_i} |.$$

If the entry location i is inside of E_t , according to Proposition A.1, there exists an optimal entry value \hat{v}_i resulting in a smaller or equal backdoor loss compared to v_i . In this case, we save i as one of entry location in \hat{E}_t .

If the entry location i is outside of E_t , we have the following observation:

For any entry location j inside of E_t , we already know

$$| \frac{\partial L(x, y_t)_{k=0}}{\partial x_i} | \geq | \frac{\partial L(x, y_t)_{k=0}}{\partial x_j} |.$$

We use Gradient Descent optimization algorithm to decrease loss by updating the entry value of the selected location with a constant step size Δv . When the selected location is i , the updated loss $L(x^i, y_t)_{k=1}$ will be

$$L(x^{\{i\}}, y_t)_{k=1} = L(x, y_t)_{k=0} - \frac{\partial L(x, y_t)_{k=0}}{\partial x_i} \Delta v,$$

and when the selected location is j , it is

$$L(x^{\{j\}}, y_t)_{k=1} = L(x, y_t)_{k=0} - \frac{\partial L(x, y_t)_{k=0}}{\partial x_j} \Delta v.$$

It can be found that

$$L(x^{\{i\}}, y_t)_{k=1} \leq L(x^{\{j\}}, y_t)_{k=1}.$$

Therefore, i is a better entry location in reducing backdoor loss compared to j when we constrain the updating step size Δv being static. After repeating the optimization step iteratively, if we finally find the optimal entry value \hat{v}_i resulting in a smaller backdoor loss compared to \hat{v}_j , then it must also outperform the fixed value v_j in V_t according to Proposition A.1. If so, we save i as one of entry location in \hat{E}_t . Otherwise, we save j as one of location in \hat{E}_t .

By recursively operating the procedures across $k = 2, 3, \dots$, we will finally construct a \hat{E}_t in which every entry location is proved to contribute a better attack performance than entry locations defined in E_t . \square

B Descriptions of Defenses

We implement our attack on FL systems integrated with 9 different defense strategies and provide a brief introduction for each of them:

FedAvg [21], a basic aggregation rule in FL, computes global model updates by averaging all clients’ model updates. Despite its effectiveness on the main task, it is not robust enough to defend against backdoor attacks in the FL system.

Median [36], a simple but robust alternative to FedAvg, constructs the global model updates by taking the median of the values of model updates across all clients

Trimmed Mean [36], in our implementation, excludes the 40% largest and 40% smallest values of each parameter among all clients’ model updates and takes the mean of the remaining 20% as the global model updates.

Krum [4] identifies an honest client whose model updates have the smallest Euclidean distance to all other clients’ model updates and takes this honest client’s model updates as the global model updates. Despite its robustness to prevent the FL system from being compromised by a minor number of adversaries, Krum is not able to ensure the convergence performance of the FL system on its main task when the data distribution of clients is highly non-IID.

RFA [23] computes a geometric median of clients’ model updates and assigns weight factors to clients depending on their distance from the geometric median. Subsequently, it computes the weighted average of all

clients’ model updates to generate the global model updates.

FLAIR [27] assigns different weight factors to clients according to the similarity of the coefficient signs between client model updates and global model updates of the previous round, and then takes the weighted average of all clients’ model updates to form the global model updates. FLAIR requires the knowledge of exact number of malicious clients existing in the FL system.

FLCert [7] randomly clusters clients, calculates the median of model updates within each cluster, incorporates them into the previous round’s global model, and derives the majority inference outcome from these cluster-updated global models as the final inference result for the entire FL system. In our implementation, we cluster clients into 5 groups, use FLCert inference outcome for testing the Attack Success Rate, and employ Median as the aggregation rule for updating the global model in each round.

FLAME [22] first clusters clients’ model updates according to their cosine similarity to each other, and then aggregates the clipped model updates within the largest cluster as the global model updates.

FoolsGold [11] reduces aggregation weights of a set of clients whose model updates constantly exhibit high cosine similarity to each other.

C Visualization of Triggers

C.1 Different types of trigger on images

We displayed different types of triggers on images from the Tiny ImageNet dataset in Figures 7, 5, and 6. The pattern of the FT trigger remains consistent across all datasets. The DFT triggers shown in Figure 6 are the same as those used for images from the CIFAR10 dataset, while for the Fashion MNIST and FEMNIST datasets, DFT triggers appear in black.

C.2 DPOT triggers on images from different datasets.

We displayed DPOT triggers generated for images from different dataset in Figure 8. Our triggers are in a small size that could not obscure important details of any images.

C.3 A3FL trigger on images of CIFAR10

In Figure 9, we showed triggers generated by A3FL’s methods on images from CIFAR10.

D Main-task Accuracy Results

Table 8 lists the Main-task Accuracy of each experiment in getting results in table 6. “None” represents no attack

existing in the FL training.

Table 9 lists Main Task Accuracy (MA) corresponding to each experiment in table 7. “None” represents no attack existing in the FL training.

Figure 5: FT trigger on Tiny ImageNet data. Training Data 5a and 5b are from different malicious clients. Test Data 5c is used to test ASR.

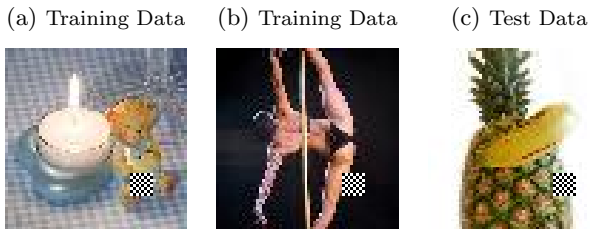


Figure 6: DFT trigger on Tiny ImageNet data. Training Data 6a and 6b are from different malicious clients. Test Data 6c is used to test ASR.

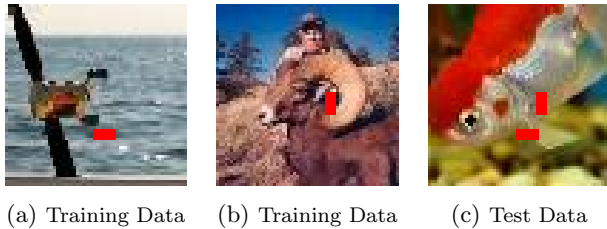


Figure 7: DPOT trigger on Tiny ImageNet data. Training Data 7a and 7b are from different malicious clients. Test Data 7c is used to test ASR.





Fashion MNIST



FEMNIST



CIFAR10



Tiny ImageNet

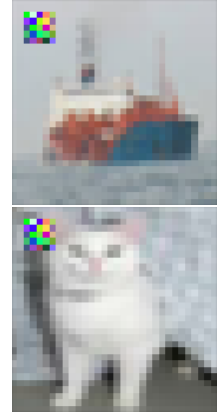


Figure 9: A3FL trigger on images from CIFAR10.

Figure 8: DPOT triggers on images from different datasets.

MCR	None	0.05			0.1			0.2			0.3		
		Ours	FT	DFT	Ours	FT	DFT	Ours	FT	DFT	Ours	FT	DFT
FedAvg	70.3	70.66	70.37	71.37	70.03	71.04	70.13	69.9	70.39	71.18	70.25	70.69	70.24
Median	70.21	69.06	69.76	69.71	69.32	69.17	70.12	68.23	69.05	68.87	68.49	68.47	67.82
Trimmed Mean	69.43	70.42	70.24	70.84	69.9	69.17	69.78	69.33	69.19	69.8	69.23	68.83	68.02
RFA	70.42	70.69	70.27	70.77	70.35	70.44	70.16	70.72	70.33	69.56	70.09	69.72	69.37
FLAIR	70.25	70.62	71.04	70.42	69.80	71.45	70.89	71.85	71.20	71.16	71.26	69.74	70.99
FLCert	69.6	69.95	69.76	70.42	69.44	69.44	69.45	69.28	69.25	69.73	68.54	69.06	68.24
FLAME	70.14	70.28	70.93	70.85	69.62	70.87	71.01	70.71	70.4	70.58	69.19	71.45	70.52
FoolsGold	70.42	71.02	71.19	71.68	70.71	71.32	71.27	70.45	70.38	70.82	70.12	69.97	69.97
Krum	47.16	41.94	35.87	49.67	41.49	33.4	38.93	40.48	41.53	44.11	41.1	34.85	40.72

Table 8: The effects of malicious client ratio on the stealthiness of different attacks (CIFAR10).

Trigger Size	None	9			25			49			100		
		Ours	FT	DFT	Ours	FT	DFT	Ours	FT	DFT	Ours	FT	DFT
FedAvg	70.3	70.88	70.72	71.25	70.66	70.37	71.37	70.77	71.35	70.94	69.92	70.71	71.15
Median	70.21	68.31	70.04	68.69	69.06	69.76	69.71	69.95	70.54	70.56	69.88	70.3	70.86
Trimmed Mean	69.43	69.75	70.13	70.19	70.42	70.24	70.84	69.42	70.17	69.79	69.67	70.26	70.68
RFA	70.42	70.45	70.16	71	70.7	70.3	70.8	70.56	70.19	70.62	70.52	69.22	70.77
FLAIR	70.25	70.79	70.67	70.58	70.62	71.04	70.42	70.84	69.96	71.03	71.17	70.65	70.28
FLCert	69.6	69.88	69.64	69.87	69.95	69.76	70.42	67.77	69.83	70.08	68.81	70.81	70.41
FLAME	70.14	70.07	71.24	70.19	70.28	70.93	70.85	69.87	71.2	70.68	67.24	71.06	70.75
FoolsGold	70.42	70.4	72.1	70.09	71.02	71.19	71.68	70.66	70.75	71.38	69.84	71.06	71.64
Krum	47.16	46.95	50.18	43.07	41.94	35.87	49.67	40.86	40.9	47.59	42.55	39.92	44.06

Table 9: The effects of trigger size on the stealthiness of different attacks (CIFAR10).